Journal of Physical Science and Application 6 (6) (2016) 49-56
doi: 10.17265/2159-5348/2016.06.007

Computational Analysis of Nanofluid Mixed Convection in a Ventilated Enclosure with Linearly Varying Wall Temperature

Ismail Arroub[1], Ahmed Bahlaoui[1], Abdelghani Raji[2], Mohammed Hasnaoui[3] and Mohamed Naïmi[2]

1. Sultan Moulay Slimane University, Polydisciplinary Faculty, Interdisciplinary Laboratory of Research in Sciences and Technologies (LIRST), B.P. 592, Béni-Mellal 23000, Morocco

2. Sultan Moulay Slimane University, Faculty of Sciences and Technologies, Laboratory of Flows and Transfers Modelling (LAMET), B.P. 523, Béni-Mellal 23000, Morocco

3. Cadi Ayyad University, Faculty of Sciences Semlalia, Laboratory of Fluid Mechanics and Energetics (LMFE), B.P. 2390, Marrakech, Morocco

Abstract: The characteristic of flow and heat transfer of Al_2O_3-water nanofluids flowing through a horizontal ventilated cavity is investigated numerically. The bottom wall is subjected to a linearly varying increasing heating temperature profile, whereas the other boundaries are assumed to be thermally insulated. The enclosure is cooled by an injected or sucked imposed flow. The simulations are focused specifically on the effects of different key parameters such as Reynolds number, $200 \leq Re \leq 5{,}000$, nanoparticles concentration, $0 \leq \phi \leq 0.1$, and mode of imposed flow, on the flow and thermal patterns and heat transfer performances. The findings demonstrate clearly the positive role of the nanoparticles addition on the improvement of the heat transfer rate and the mean temperature within the cavity. Also, the results presented show that, the suction mode is more favorable to the heat transfer in comparison with the case of the injection mode. The cooling efficiency is found to be more pronounced by applying the suction mode.

Key words: Mixed convection, nanofluid, injection, suction, linearly varying heating, ventilated cavity.

1. Introduction

The study of mixed convection receives a considerable attention because of its wide and practical applications in real world engineering concerns. These concerns can be observed in various fields such as cooling of electronic and electrical equipments, room cooling, air conditioning, drying, grains and food processing, solar heating, nuclear reactor and combustion chambers. In the other hand, fluids such as water, oil or ethylene glycol are frequently encountered in industrial applications, but only have a low thermal conductivity compared to that of crystalline solids. The idea is to insert within the fluid, metallic particles of nanometer size in order to increase the effective thermal conductivity of the mixture (nanofluid) which can be achieved even at very low volume fraction of nanoparticles. Consequently, the presence of the nanoparticles in the base fluids enhances the heat transfer characteristics of nanofluids [1, 2]. Nevertheless, the nanofluids' thermal conductivity could be affected by many parameters such as volume fraction of suspended nanoparticles, their type, their size and shape, the nature of the base fluid and the temperature of the medium [3]. In this context, many different configurations and combinations of thermal boundary conditions have been considered and analyzed by various investigators.

Some studies were focused on mixed convection

Corresponding author: Ahmed Bahlaoui, Ph.D., professor, research fields: heat and mass transfer, fluid mechanics.

flow in a lid-driven cavity. Among the recently published works, we quote those by Kefayati [4] dealing with mixed convection of non-Newtonian aluminum-water nanofluids by using finite difference Lattice-Boltzmann method. From this study, it is observed that the effect of nanoparticles on the enhancement of heat transfer decreases with increase in power-law index. Also, the influence of nanoparticles for different power-law indexes drops as the Richardson number augments. Another study concerning a comparative numerical study on the effects of uniform (isothermal) and non-uniform (sinusoidal) heating of bottom wall in a heat generating nanofluid filled with lid-driven cavity has been performed by Muthtamilselvan and Doh [5]. The results reveal that the non-uniform heating condition attains maximum heat transfer rates at the center of the bottom wall than with uniform heating condition for all Richardson number. Moreover, it is obtained that the nanoparticles are able to change the flow patterns of a fluid from mixed convection to forced convection regime for $\mathrm{Ri} \geq 1$.

Mixed convection of nanofluids in ventilated cavities has been also the object of interest during the last years. In this perspective, the problem of mixed convection flows through an alumina-water nanofluid in a square cavity heated by imposed uniform temperature, with incoming flow oscillation was performed by Sourtiji et al. [6] for the Top-Bottom configuration. It is reported that the presence of the nanoparticles in the base fluid cased to increase the pressure drop coefficient in the cavity due to the more viscosity of the nanofluid and enhances the heat transfer for all the investigated Strouhal and Richardson numbers. The same authors (Sourtiji et al. [7]), considered the case where the incoming flow is steady and the inlet port is located on the upper part of the left wall whereas the location of the outlet port was varied along the four walls. They concluded that the maximum value of Nusselt number is obtained when the outlet port is placed in any one of the three corners. Moreover, the results showed that an enhancement in the heat transfer and pressure drop is observed by adding the nanoparticles to the base fluid.

In the case of a cavity cooled by an injected or sucked imposed flow, the problem of mixed convection flows through an alumina-water nanofluid in a vented horizontal cavity heated from below was performed numerically by Bahlaoui et al. [8]. They reported that the enhancement of heat transfer across the cavity and the increase of the average temperature inside the enclosure due to the presence of nanoparticles are more pronounced in both the injection and suction modes. Recently, the same authors (Bahlaoui et al. [9]) have extended the study by considering a vertical cavity heated from one side. They found that the suction mode is more efficient than the injection mode by leading to more heat transfer across the cavity and a better cooling of the cavity is reached with the suction mode.

To the best knowledge of the authors, the problem of mixed convection of nanofluids in a cavity ventilated by two different modes and heated with a linearly varying hot temperature profile has not been analyzed. Such physical model may be encountered in a number of cooling industrial applications. Therefore, the present work aims to examine the effects of the main parameters such as the Reynolds number, the nanoparticles concentration and the mode of imposed forced flow (injection or suction) on the flow and energy fields.

2. Problem Description and Mathematical Formulation

Consider a steady, laminar, mixed convection in an incompressible Al_2O_3-water nanofluid from a ventilated cavity with an aspect ratio $A = 2$. The cavity is subjected to an injected (Fig. 1a) or sucked (Fig. 1b) imposed external flow entering the cavity from the left-bottom opening and leaving from the right-upper one. These openings have a constant relative dimension, $B = 1/4$. The bottom wall is heated by a linearly varying hot temperature (see Fig. 1c) and the remaining boundary parts of the enclosure are adiabatic. Thus, it is assumed that both the fluid phase and nanoparticles are in thermal equilibrium and the shape and size of solid particles are assumed to be uniform. Also, the thermo-physical properties of the nanofluid are constant except for the density variation, which is approximated by the *Boussinesq* model.

Therefore, using the following dimensionless variables:

$A = L'/H'$, $B = h'/H'$, $x = x'/H'$, $y = y'/H'$, $u = u'/u'_o$, $v = v'/u'_o$, $t = t'u'_o/H'$, $T = (T' - T'_C)/(T'_H - T'_C)$, $\Psi = \Psi'/u'_o H'$, $\Omega = \Omega' H'/u'_o$, $Pr = \nu_f/\alpha_f$, $Ra = g\,\beta_f (T'_H - T'_C) H'^3/\alpha_f \nu_f$, $Re = u'_o H'/\nu_f$

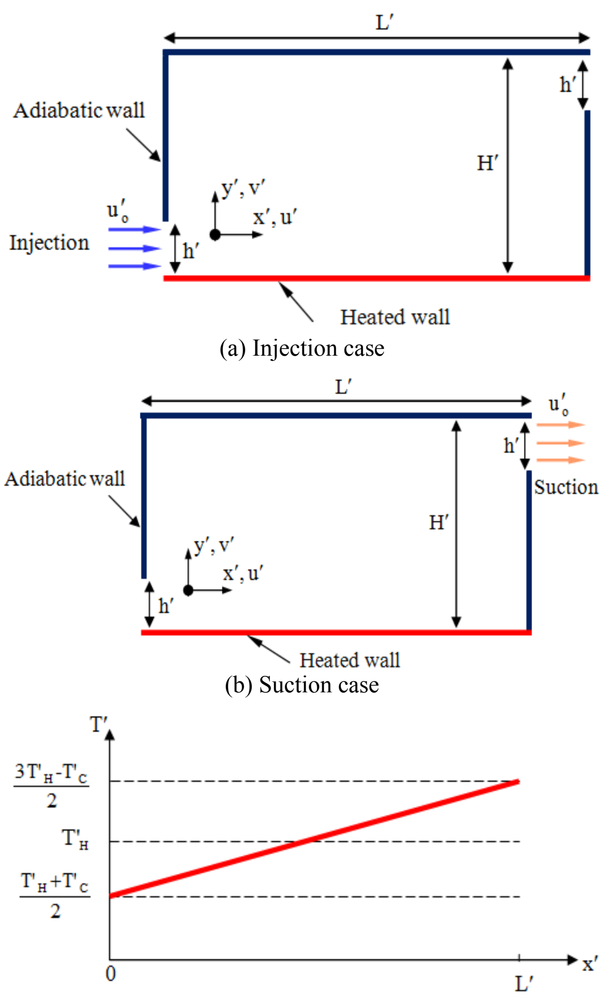

(a) Injection case

(b) Suction case

(c) Imposed temperature profile on the heated wall

Fig. 1 Geometry and coordinate system: a) Injection case, b) Suction case and c) Heating temperature profile.

the momentum, energy and continuity equations using the vorticity-stream function (Ω-Ψ) formulation can be written in the non-dimensional form as follows:

$$\frac{\partial\Omega}{\partial t}+u\frac{\partial\Omega}{\partial x}+v\frac{\partial\Omega}{\partial y}=\frac{Ra}{Re^2 Pr}\left[\left(\frac{\varphi}{\left((1-\varphi)\frac{\rho_f}{\rho_s}+\varphi\right)}\right)\frac{\beta_s}{\beta_f}+\frac{1}{\left(\frac{\varphi}{(1-\varphi)}\frac{\rho_s}{\rho_f}+1\right)}\right]\frac{\partial T}{\partial x}$$
$$+\frac{1}{Re}\left[\frac{1}{(1-\varphi)^{2.5}\left(\varphi\frac{\rho_s}{\rho_f}+(1-\varphi)\right)}\right]\left(\frac{\partial^2\Omega}{\partial x^2}+\frac{\partial^2\Omega}{\partial y^2}\right) \quad (1)$$

$$\frac{\partial T}{\partial t}+u\frac{\partial T}{\partial x}+v\frac{\partial T}{\partial y}=\frac{1}{Re\,Pr}\left(\frac{\frac{\lambda_{nf}}{\lambda_f}}{(1-\varphi)+\varphi\frac{(\rho c_p)_s}{(\rho c_p)_f}}\right)\left(\frac{\partial^2 T}{\partial x^2}+\frac{\partial^2 T}{\partial y^2}\right) \quad (2)$$

$$\frac{\partial^2\Psi}{\partial x^2}+\frac{\partial^2\Psi}{\partial y^2}=-\Omega \quad (3)$$

The dimensionless tangential and normal velocities are converted to:

$$u=\frac{\partial\Psi}{\partial y}\ ;\ v=-\frac{\partial\Psi}{\partial x}\ \text{ and }\ \Omega=\frac{\partial v}{\partial x}-\frac{\partial u}{\partial y} \quad (4)$$

Nanofluid effective density, effective thermal conductivity, thermal diffusivity, heat capacity and the thermal expansion coefficient are, respectively, calculated as follow:

$$\rho_{nf}=\phi\rho_s+(1-\phi)\rho_f \quad (5)$$

$$\frac{\lambda_{nf}}{\lambda_f}=\frac{\lambda_s+2\lambda_f-2\phi(\lambda_f-\lambda_s)}{\lambda_s+2\lambda_f+\phi(\lambda_f-\lambda_s)} \quad (6)$$

$$\alpha_{nf}=\frac{\lambda_{nf}}{(\rho c_p)_{nf}} \quad (7)$$

$$(\rho c_p)_{nf}=\phi(\rho c_p)_s+(1-\phi)(\rho c_p)_f \quad (8)$$

$$(\rho\beta)_{nf}=\phi\rho_s\beta_s+(1-\phi)\rho_f\beta_f \quad (9)$$

Where "*f*", "*s*" and "*nf*" indicate fluid, solid particles and nanofluid respectively.

2.1 Boundary Conditions

The common boundary conditions applied to the two ventilation modes would be adjusted as follows:

$u = v = 0$ on the rigid walls

$T = \frac{x}{A} + \frac{1}{2}$ on the lower horizontal heated wall

$\frac{\partial T}{\partial n} = 0$ on the adiabatic walls

$\Psi = 0$ on the walls below the two openings

$\Psi = B$ on the walls above the two openings

The appropriate boundary conditions associated to each mode are given in the subsequent sections

Injection case:

$T = 0,\ \Psi = y,\ \Omega = 0,\ u = 1,\ v = 0$ at the inlet port

Suction case:

T = 0 at the inlet port

$u = 1, v = 0, \Psi = y - (1 - B), \Omega = 0$ at the outlet port

"n" indicates the normal direction to the considered adiabatic wall.

2.2 Heat Transfer

The rate of heat removal from the heating element is expressed in terms of average Nusselt number, Nu, calculated on the heated bottom wall of the cavity, which is defined by:

$$Nu = -\frac{1}{A}\left(\frac{\lambda_{nf}}{\lambda_f}\right)\int_0^A \left.\frac{\partial T}{\partial y}\right|_{y=0} dx \qquad (10)$$

3. Numerical Procedure

The two-dimensional governing equations, (1)-(3), are solved by using the finite difference method with a regular mesh size. The advection terms are approximated by the second-order upwind differencing scheme which leads to a stable solution. Also, the second-order central differencing scheme is utilized to approximate the diffusive terms. The integration of the vorticity and energy equations, (1) and (2), is performed with the ADI (alternating-direction implicit) method. To satisfy the mass conservation, the Poisson equation, (3), is solved by a PSOR (point successive over-relaxation) method with an optimum over-relaxation factor equal to 1.95 for the grid (201 × 101) retained in this work.

4. Results and Discussion

In this part, the Rayleigh number was kept fixed at Ra = 10^6 and the Reynolds number varying in the range $200 \leq Re \leq 5{,}000$. It is worth noting that the generated values of Richardson number, Ri, are varied from 6.45×10^{-3} to 4.03 to cover natural convection, mixed convection and forced convection dominating regimes. In the following, effects of solid volume fraction, Reynolds number and imposed flow mode through the cavity on flow and thermal fields and on heat transfer effectiveness are explored. Before dealing with this exhibition results, it is to indicate that the flow is unsteady as *Re* is very weak. Therefore, the dynamical and thermal structures could not be presented in this situation.

Streamlines and isotherms plots illustrating the effect of Re on the dynamical and thermal fields, for the injection case, are shown in Figs. 2a-2d for both $\phi = 0$ (solid line —) and $\phi = 0.1$ (dashed line - - -). For a moderate value of Re (Re = 700), the streamlines show the presence of two closed cells separated by the open lines of the forced flow (Fig. 2a). More precisely, a big trigonometric cell, engendered by shear effects, is located in the upper part of the cavity while the small clockwise one, due to combined effects of free convection and shear is located below the open lines, in contact with the heated wall. A very limited qualitative effect can be observed in the flow structure by increasing ϕ from 0 to 0.1, if we except the small cell located below the open lines; the size of the latter is increased and its center is shifted to the right. The corresponding isotherms show that heat exchange between the linearly heated surface and the nanofluid is restricted to the area limited by the active boundary and the vertical right one due to the closed convective cell. On the other hand, for the half of the cavity (there where the closed cells are generated by the shear effects), the fluid is at a uniform cold temperature. In fact, the existence of this cold region indicates the absence of thermal interaction between the active wall and the working fluid in the area above the diagonal

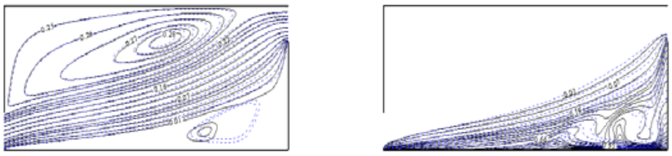

(a) *Re* = 700

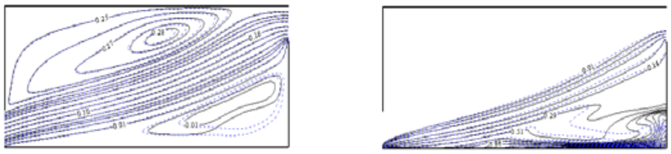

(b) *Re* = 1000

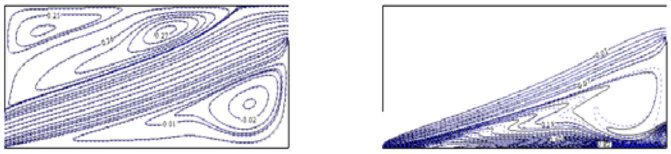

(c) *Re* = 2000

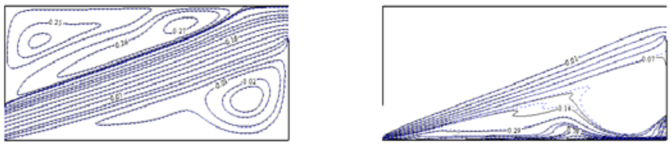

(d) *Re* = 5000

Fig. 2 Streamlines and isotherms, in the injection mode, for $\phi = 0$ (—) and $\phi = 0.1$ (- - -) at different values of *Re*: a) *Re* = 700, b) *Re* = 1,000, c) *Re* = 2,000 and d) *Re* = 5,000.

linking the cavity openings. In addition, the isotherms corresponding to the nanofluid (with $\phi = 0.1$) are not consistent with the case of pure fluid ($\phi = 0$) at the right side of the bottom wall. They are well stratified and dispersed along the thermal boundary layer. This behavior is explained by a good heat exchange between the heated wall and the open lines through the small cell and also the temperature homogenization within the cavity in the case of nanofluid. More increase of Re up to 1,000 leads to an increase of the size and intensity of the lower cell which is evidently supported by the increase of the forced convection effect (Fig. 2b). A further increase of Re up to 2,000 then to 5,000 (dominating forced convection regime) promotes the lower cell as shown in Figs. 2c-2d. This promotion in terms of size occurs to the detriment of the space allowed in the lower part of the cavity. In the meantime, the upper cell undergoes a split into two others ones due to the large shear effect resulting from the growing forced convection role. Furthermore, the forced convection dominated regime engenders the shape of the open lines which become straight and parallel between the two openings. The corresponding isotherms show that all isotherms are condensed near the heating wall, which indicates that the heat provided by the isothermal wall is transported by the forced flow directly towards the outlet without ensuring a good interaction with the closed cells. Also, as expected, thermal and dynamical structures become insensitive to the nanoparticles concentration for large values of Re.

The effect of Re on the streamlines and isotherms is illustrated in Figs. 3a-3d for both pure water and the Al_2O_3-water nanofluid in the case of suction mode. For Re = 700 (Fig. 3a), the flow structure shows the existence of three closed cells. Two cells mainly generated by the shear effect are located above the forced flow lines and one clockwise cell below the open lines is located in the space surrounding the lower right corner of the cavity. This negative cell is generated by aiding combined effects of buoyancy and shear. For this case, the open lines are curved and regular. Also, these forced lines interact better with the heating wall. This observation is confirmed by the corresponding isotherms where we can observe important temperature gradients along the heated wall. In addition, Fig. 3a shows that the cold front invades almost three quarters of the cavity. A regular increase of Re to 1,000, 2,000 and 5,000, cases illustrated in Figs. 3b to 3d respectively, leads qualitatively to the same flow structure. It is however observed that this increase is more favorable to the cells located in the vicinity of the opposite corners of the cavity and unfavorable to the shear cell in contact with the open lines. The grow of the negative cell accompanying the increase of Re results from the positive role of this parameter in promoting the assisting effects between natural and forced convections. In addition, the amplification of the size of the closed cell located in the left top corner of the cavity occurs to the detriment of the positive cell in contact with the open lines.

It is to underline that, even for large values of Re, the curved shape of the open lines is maintained. However, the latter are visibly more and more detached from the first half of the heating wall as Re increases. This detachment is obviously amplified by the extension of the negative cell promoted by the increase of Re. The isotherms show a good heat exchange between the active wall and the fluid throughout its surface. The improvement of this exchange is in fact promoted by the increase of Re since the latter parameter is favorable to the development of the negative cell which interacts directly with the most heated part of the wall.

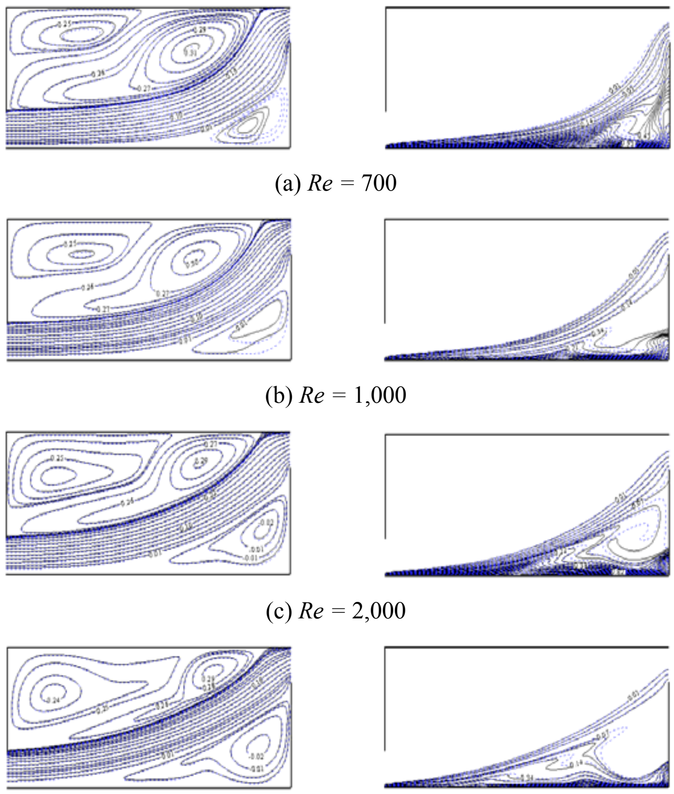

(a) Re = 700

(b) Re = 1,000

(c) Re = 2,000

(d) Re = 5,000

Fig. 3 Streamlines and isotherms, in the suction mode, for ϕ = 0 (—) and ϕ = 0.1 (- - -) at different values of Re: a) Re = 700, b) Re = 1,000, c) Re = 2,000 and d) Re = 5,000.

In order to illustrate the performance of the injection and suction modes in the heat removal, variations versus the Reynolds number of the mean Nusselt number, Nu, along the hot wall are presented in Fig. 4 for different values of ϕ. In the case of the suction mode, a monotonous increase of Nu with Re is observed with a constant rate for the considered range of Re. For the injection mode, it can be noted that a value of Nu remains constant if we increase Re up to 500. Then, a slight decrease of Nu with Re is observed up to a critical value, $Re_{CR} \approx 1{,}000$. This decrease of the mixed convection effect, occurring in the transition phase toward the forced flow regime, is attributed to the increase of the size of the closed cell between the heated wall and the open lines and consequently the delaying of heat released by the hot wall towards outside through the open lines (Figs. 2a-2b). Beyond this threshold value of Re, the tendency is reversed. The evolution of Nu is then characterized by a monotonic increase with Re resulting from an enhanced thermal interaction between the heated wall and the dominant forced flow. This singularity is absent in the suction mode because the forced flow remains completely or partially in direct contact with the hot wall what involves a continuous increase in Nu with Re. For a fixed value of Re, the increase of the solid volume fraction ϕ up to 0.1 leads to a noticeable growing effect of the convection in both the injection and suction cases. This is due to the increase in effective thermal conductivity of the nanofluid with the increase in ϕ. More precisely, by increasing ϕ from 0 to 0.1, Nu is increased for the more favorable case, obtained for Re = 5,000, from 27.63/(27.22) to 32.32/(31.77) for the suction/injection mode respectively. It should be noted that, in comparison with the injection mode, the suction mode enhances the heat transfer more, and consequently permits better cooling within the cavity for all Re values ranging from 200 to 5,000 in both the cavity filled with pure fluid (water) and nanofluid cases. Hence, in both injection and suction modes, unsteady solutions are encountered, when the Reynolds number is lower than a critical value (which depends on Ra and other parameters) and the Rayleigh number is high enough. These periodic solutions are indicated by solid circles in Fig. 4. Their existence is limited in the range of $200 \le Re \le 600$/($200 \le Re \le 700$) for the suction/(injection) mode respectively, depending on ϕ.

For practical purposes, the evaluation of mean temperature of the nanofluid inside the cavity is of a great importance. Thus, variations of this quantity with Re are plotted in Fig. 5 for different values of ϕ for both the injection and suction modes. In particular, in the injection case the average temperature $\overline{T}$ increases by increasing Re up to a critical value ranging from 800 to 1,000, which strongly depends on

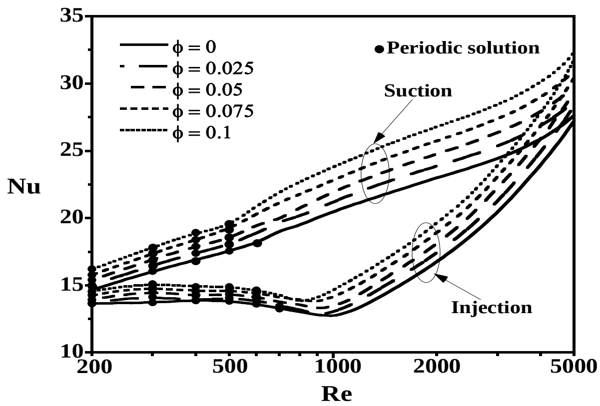

Fig. 4 Variations, with *Re*, of the average Nusselt number, *Nu*, in both injection and suction modes for various values of ϕ.

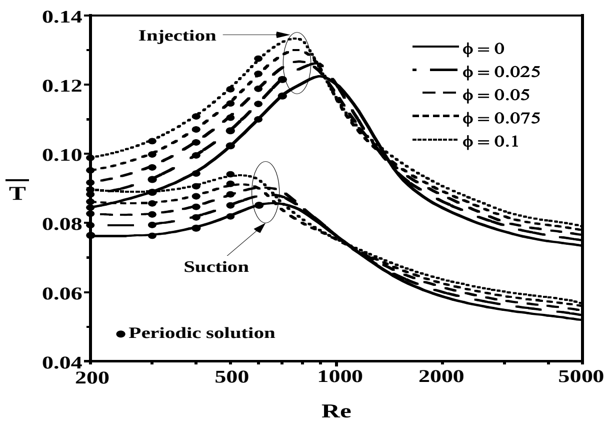

Fig. 5 Variations, with *Re*, of the mean temperature, $\overline{T}$, in both injection and suction modes for various values of ϕ.

ϕ. This reheating of the cavity is justified by the constant heat transfer in this range of Re (see Fig. 4 for the injection case). Then, this tendency is reversed because the growing of Re is marked by a decrease in $\overline{T}$; this behavior is due to the forced convection predominant effect, which drives the heat toward the outside and thereafter contributes to the cooling of the cavity. For the other case (suction), it can be noted that the increase of $\overline{T}$ with Re remains very limited as long as Re is almost lower than 600. Above this threshold, the evolution of mean temperature $\overline{T}$ with Re is characterized by a continuous decrease. It is obvious from this figure that for a given value of Re, the average temperature increases when solid concentration increases, for the two modes of imposed flow, because the presence of nanoparticles leads to a good heat exchange by convection in the cavity and contributes consequently to an increase of the average temperature. Also, it is interesting to observe that the suction mode leads to a better cooling of the cavity since the resulting values of $\overline{T}$ are lower in comparison with the injection mode. For reasons of clarity, it is noted that, for $\phi = 0.1$ and Re = 800, a reduction of about 39.40% of $\overline{T}$ occurs when passing from the injection mode to the suction one.

5. Conclusions

The salient observations obtained from the present work in regard to a vented rectangular cavity following injection and suction of Al_2O_3-water nanofluid with a linearly increasing heating are given below.

- The flow and temperature patterns are affected depending on the mode of imposed flow.
- The suspended nanoparticles contribute substantially to improve the heat transfer exchanged between the active wall and the nanofluid and to an increase of the average temperature within the cavity by applying both injection and suction modes.
- The suction mode gives a better thermal efficiency than the injection mode by leading to more heat transfer across the cavity even with or without the presence of nanoparticles, which implies that the suction mode gives a better cooling of the cavity in comparison with the injection one.

References

[1] Khanafer, K., Vafai, K., and Lightstone, M. 2003. "Buoyancy-Driven Heat Transfer Enhancement in a Two-Dimensional Enclosure Utilizing Nanofluids." *Int. J. Heat Mass Transfer* 46: 3639-53.

[2] Chandrasekar, M., Suresh, S., and Bose, A. C. 2010. "Experimental Investigations and Theoretical Determination of Thermal Conductivity and Viscosity of Al_2O_3/Water Nanofluid." *Experimental Thermal and Fluid Science* 34: 210-6.

[3] Haddad, Z., Oztop, H. F., Abu-Nada, E., and Mataoui, A. 2012. "A Review on Natural Convective Heat Transfer of Nanofluids." *Renewable and Sustainable Energy Reviews* 16: 5363-78.

[4] Kefayati, G. H. R. 2014. "Mixed Convection of Non-Newtonian Nanofluids Flows in a Lid-Driven Enclosure with Sinusoidal Temperature Profile Using FDLBM." *Powder Technology* 266: 268-81.

[5] Muthtamilselvan, M., and Doh, D. H. 2014. "Mixed Convection of Heat Generating Nanofluid in a Lid-Driven Cavity with Uniform and Non-uniform Heating of Bottom Wall." *Applied Mathematical Modelling* 38 (13): 3164-74.

[6] Sourtiji, E., Hosseinizadeh, S. F., Bandpy, M. G., and Ganji, D. D. 2011. "Effect of Water-Based Al_2O_3 Nanofluids on Heat Transfer and Pressure Drop in Periodic Mixed Convection inside a Square Ventilated Cavity." *Int. Comm. Heat Mass Transfer* 38 (8): 1125-34.

[7] Sourtiji, E., Bandpy, M. G., and Ganji, D. D., Hosseinizadeh, S. F. 2014. "Numerical Analysis of Mixed Convection Heat Transfer of Al_2O_3-Water Nanofluid in a Ventilated Cavity Considering Different Positions of the Outlet Port." *Powder Technology* 262: 71-81.

[8] Bahlaoui, A., Raji, A., Hasnaoui, M., and Naïmi. M. 2014. "Mixed Convection in a Nanofluid-Filled Vented Rectangular Cavity: Suction and Injection Heat Performance." *Computational Thermal Sciences* 6 (2): 129-42.

[9] Bahlaoui, A., Raji, A., Hasnaoui, M., and Naïmi. M. 2016. "Mixed Convection Heat Transfer Enhancement in a Vented Cavity Filled with a Nanofluid." J*ournal of Applied Fluid Mechanics* 9 (2): 593-604.